# Analysis of the Treadmilling Model during Metaphase of Mitosis Using Fluorescence Redistribution After Photobleaching

Patricia Wadsworth and E. D. Salmon

Department of Biology, University of North Carolina, Chapel Hill, North Carolina 27514. Dr. Wadsworth's present address is Department of Zoology, University of Massachusetts, Amherst, Massachusetts 01003.

*Abstract.* One recent hypothesis for the mechanism of chromosome movement during mitosis predicts that a continual, uniform, poleward flow or "treadmilling" of microtubules occurs within the half-spindle between the chromosomes and the poles during mitosis (Margolis, R. L., and L. Wilson, 1981, *Nature (Lond.)*, 293:705–711). We have tested this treadmilling hypothesis using fluorescent analog cytochemistry and measurements of fluorescence redistribution after photobleaching to examine microtubule behavior during metaphase of mitosis. Mitotic BSC 1 mammalian tissue culture cells or newt lung epithelial cells were microinjected with brain tubulin labeled with 5-(4,6-dichlorotriazin-2-yl) amino fluorescein (DTAF) to provide a fluorescent tracer of the endogenous tubulin pool. Using a laser microbeam, fluorescence in the half-spindle was photobleached in either a narrow 1.6 μm wide bar pattern across the half-spingle or in a circular area of 2.8 or 4.5 μm diameter. Fluorescence recovery in the spindle fibers, measured using video microscopy or photometric techniques, occurs as bleached DTAF-tubulin subunits within the microtubules are exchanged for unbleached DTAF-tubulin in the cytosol by steady-state microtubule assembly-disassembly pathways. Recovery of 75% of the bleached fluorescence follows first-order kinetics and has an average half-time of 37 sec, at 31–33°C. No translocation of the bleached bar region could be detected during fluorescence recovery, and the rate of recovery was independent of the size of the bleached spot. These results reveal that, for 75% of the half-spindle microtubules, FRAP does not occur by a synchronous treadmilling mechanism.

THE dynamic non-steady-state behavior of spindle microtubules in living cells has been clearly demonstrated by a variety of experimental approaches. For example, the majority of spindle fiber birefringence can be rapidly and reversibly abolished by cold, high-pressure, or anti-mitotic drugs (28). Spindle birefringence disappears uniformly throughout the half-spindle, primarily due to the depolymerization of non-kinetochore microtubules. Kinetochore microtubules, usually a small fraction of the total number of microtubules in the half-spindle, are differentially stable to such treatments (3, 25, 30).

More recently, the steady-state behavior of spindle microtubules has been studied using the techniques of fluorescence analog cytochemistry (40) and fluorescence redistribution after photobleaching (FRAP)[1] (1, 12, 14, 43). These studies have demonstrated that steady-state tubulin subunit exchange with the majority of spindle microtubules is remarkably rapid. In these experiments, mitotic tissue culture cells or sea urchin embryos were microinjected with fluorescein-labeled tubulin (13, 16, 42) to serve as a tracer of the endogenous tubulin pool. Fluorescent tubulin incorporated into spindle fibers rapidly, uniformly, and to near steady-state levels within 60 s (8, 33, 34). When a brief, intense pulse of laser light was then used to irradiate a restricted, defined area in a fluorescent half-spindle, the fluorophores bound to tubulin in that region were permanently bleached (33, 34). Recovery of fluorescence was observed as unbleached 5-(4,6-dichlorotriazin-2-yl) amino fluorescein (DTAF)–tubulin molecules within the cytosol exchanged with bleached molecules in spindle fibers, at steady-state. The recovery of fluorescence in circular spot bleaches in the half-spindle was rapid, apparently uniform, exponential (half-time = 10–24 s), and nearly complete at physiological temperatures (33, 34). Mitosis continued normally (33, 34). The use of DTAF–tubulin as a probe for tubulin incorporation into microtubule polymer in vivo and the absence of detectable microtubule destruction by laser photobleaching have been recently demonstrated (for review see references 16, 21, 33, 34). Results of control experiments include the following: (*a*) DTAF–tubulin assembles only onto the ends of axonemal microtubules and does not bind to the axonemal wall (16); (*b*) fluorescence of the spindle fibers changes concurrently with the assembly of microtubules during mitosis and spindle fluorescence disappears when cells are

[1] *Abbreviations used in this paper:* ARBs, areas of reduced birefringence; DTAF, 5-(4,6-dichlorotriazin-2-yl) amino fluorescein; FRAP, fluorescence redistribution after photobleaching.

treated with microtubule-depolymerizing agents (33, 34); (*c*) photobleaching does not alter spindle birefringence (33); (*d*) the distribution of interphase microtubules is not altered by photobleaching (34); and (*e*) progress through mitosis is not affected even after multiple bleaches (33, 34). Thus, photobleaching of DTAF–tubulin (16) caused no detectable changes in the structure of spindle fibers. The recovery of fluorescence in a photobleached area, then, requires that non-irradiated, unbleached DTAF–tubulin molecules exchange with bleached subunits in the spindle fiber microtubules by steady-state assembly/disassembly pathways.

In the experiments reported here, we have used the FRAP technique to test the major prediction of the treadmilling model for mitosis. The treadmilling model is based on the opposite-end assembly and disassembly of microtubules measured in vitro (18). The model predicted that microtubules in each half-spindle, both kinetochore and nonkinetochore, would be of uniform polarity (2): plus (+) ends distal to the spindle pole and minus (−) ends proximal to the spindle pole, which has been verified experimentally (5, 41). Furthermore, the model suggested that subunits continually assemble into microtubules at the (+) ends while disassembling at an equal rate from the (−) ends. Where nonkinetochore microtubules from opposite spindle poles overlap, they would interact laterally to generate poleward movement of microtubules in order to balance the net rate of assembly and convert tubulin subunit flux into work. Thus, all microtubules in each half-spindle would flow continuously poleward during all stages of mitosis. At the onset of anaphase, subunit association was assumed to be blocked at the kinetochore while continued disassembly of microtubules at the pole would result in a net shortening of the kinetochore fiber as the microtubules flow poleward (19, 20).

Two types of FRAP experiments were designed in an attempt to detect a uniform, poleward flow of spindle microtubules during mitosis. In the first of these experiments, the laser light was focused through a cylindrical lens, restricting the bleach to a narrow bar pattern that extended completely across the half-spindle of metaphase spindles of BSC 1 or newt lung epithelial cells. Time-lapse video micrographs of fluorescence recovery were examined to determine if the bleached region was translocated poleward as predicted by the treadmilling hypothesis. In the second type of experiment, the treadmilling model was tested by measuring FRAP in metaphase half-spindles of BSC 1 cells for circular bleach patterns of two different diameters. If FRAP is produced by a poleward flow of tubulin subunits within half-spindle microtubules, then the recovery curves will display a sigmoid shape and the rate of recovery should be inversely proportional to the beam diameter.

# Materials and Methods

## Protein Preparation

Microtubule protein was prepared from porcine brains (37, 38) and labeled with DTAF as described by Leslie et al. (16) with several minor modifications. The tubulin assembly buffer consisted of 0.1 M Pipes, 1 mM $MgSO_4$, 2 mM EGTA, and 0.5 mM GTP, pH 6.9. After labeling with DTAF, tubulin was purified by five assembly/disassembly cycles in 1 M Na-glutamate, 0.5 mM $MgSO_4$, 1 mM EGTA, and 0.2 mM GTP, pH 6.9. After the final assembly step, the DTAF–tubulin pellet was resuspended in injection buffer (20 mM Na-glutamate, 0.5 mM $MgSO_4$, 2 mM EGTA) and was frozen in liquid nitrogen at a protein concentration of 50–80 $\mu$M and stored at −80°C.

## Cell Culture

All reagents for tissue culture were obtained from Gibco (Grand Island, NY). BSC 1 cells (generous gift of B. Neighbors, University of Colorado at Boulder) were grown on 22-mm square coverslips in Dulbecco's modified Eagle's medium with 20 mM Hepes, pH 7.3, at 37°C. Primary cultures of newt (*Taricha granulosa*) lung epithelial cells were grown in 0.6 X Leibovitz's medium supplemented with 10% fetal bovine serum, 5% whole egg ultrafiltrate, and antibiotics, pH 7.25, at 25°C. Small lung fragments (~2 $mm^2$) were rinsed three times in 0.6 X Tyrodes' salt solution and held in media for 24–48 h before culturing in Rose chambers (26, 27). Cells were fed at 5-d intervals. For microinjection, the coverslips containing the explanted cells were removed from the Rose chambers and the dialysis membranes were carefully peeled away.

## Microinjection

Cells were pressure microinjected essentially as described by Graessmann et al. (7). Microneedles were pulled from Omega dot capillary tubing (Glass Company of America, Bargaintown, NJ) on a Narishige micropipette puller. Needles were back-loaded using a 10-$\mu$l Hamilton syringe; the outer diameter of the needle tip was ~0.5–1.0 $\mu$m. Cells on coverslips were injected at room temperature in culture media in 25-mm petri dishes on a Leitz Diavert microscope using a Brinkman MM 33 Compact Micromanipulator and returned to the incubator (37°C for BSC 1 cells, 25°C for newt cells) to equilibrate after injection. For the experiments reported here, coverslips containing injected cells were mounted in Rose chambers (27) for observation. Experimental temperature was maintained at 31 ± 2°C using a Sage model 279 air curtain incubator for all of the experiments with BSC 1 cells. Experiments using newt cells were performed at room temperature, usually 22°C.

## Fluorescence Microscopy, Photobleaching and Video Recording

All of the experiments reported here were performed on an inverted optical bench microscope (9) equipped as described below. For epifluorescence, a Zeiss 4 FL epi-illuminator, 100-W Hg burner, and DC-regulated power supply provided the illumination, and Zeiss fluorescein excitation and barrier filters (#487709) were used. Cells were imaged using a Zeiss 63X/1.4 NA plan apochromat. The bar bleach pattern (~1.6 $\mu$m wide) was produced by focusing a 488-nm laser beam at the field diaphragm plane of the epi-illuminator through a cylindrical lens (18-mm focal length). Bleaching was produced by a 0.1-s pulse of laser light as described below. Fluorescence images were obtained with a Venus DV2 camera and recorded by 35-mm photography of the video monitor (32). Electronic shutters (Uniblitz; Vincent Associates, Rochester, NY) limited epi-illumination during photographic exposures to 0.5 s to prevent photobleaching during recovery.

## Photometric Recording of FRAP

Fluorescence excitation and bleaching were produced by a 488-nm laser microbeam (Spectra-physics model 164), which had a circular Gaussian profile, by initially focusing the laser beam on to the field diaphragm plane of the epi-illuminator (32) using a spherical focusing lens (17.5-mm focal length). The beam cross section was constant through the spindle along the optic axis (34). The diameter of the beam at its point of focus on the specimen was determined from the relationship: $D = 1/e$ (maximum intensity of the laser beam) (1). A 25x PH Zeiss Neofluor objective produced a 4.5-$\mu$m diameter beam and a 40x PH Zeiss Neofluor produced a 2.8-$\mu$m diameter beam through the specimen. For bleaching, the laser beam power was 100 mW, attenuated by 1.8 OD using neutral density filters. During the measurement phase, the laser was further attenuated by a factor of $5 \times 10^4$ compared with the bleaching intensity by an electronic shutter (12). In control experiments, the attenuated laser beam alone did not cause detectable photobleaching. However, to ensure that the attenuated laser beam did not cause damage to living cells, the fluorescence after photobleaching was measured intermittently, not continually, using a manual shutter. Spindle fluorescence was bleached by 40–60% within a 0.1-s exposure to the unattenuated laser beam. The fluorescence image was projected through a pinhole (14) in the image plane to an EMI 9863A photomultiplier. The number of photon counts was recorded every 0.5 s using a C-10 photon counter (EMI) and an Apple II Plus computer to sample, store, and plot the data. A total of 768 data points were recorded. Five initial fluorescence values were used to normalize the fluorescence data before plotting the graphs of $\bar{F}(t)$.

## Data Analysis

The photometric data, obtained from BSC 1 spindles, for the incorporation phase of fluorescence recovery was analyzed using the first-order, perturbation–

relaxation function (33, 34): $\bar{F}(t) = \bar{F}_\infty - [\bar{F}_\infty - \bar{F}(o)]\, e^{-kt}$. Exponential regression analysis of the data was performed using the Apple II Plus computer by plotting $\ln \bar{F}_\infty - \bar{F}(t)$ vs. time after photobleaching, where $\bar{F}_\infty$ = average fluorescence at ~225 s after bleaching. For fluorescence recovery, which we found to have a half-time of ~40 s at 32°C, recovery is expected to be 97% complete 200 s after bleaching. A straight line was fit by linear regression through the data points recorded over approximately the first 80 s after bleaching. This line was used to calculate the following parameters: $k$, the first-order rate constant, was obtained from the slope of the line; and $\bar{F}(o)$, the fluorescence in the spindle fibers just after bleaching, was determined from the value of $[\bar{F}_\infty - \bar{F}(t)]$ on the straight line at the time of bleaching (t = $O$); and %R (percent recovery) = $[\bar{F}_\infty - \bar{F}(o)]/[\bar{F}_- - \bar{F}(o)]$, where $\bar{F}_-$ = average fluorescence before bleaching. From the calculated values of $\bar{F}_\infty$, $\bar{F}(o)$, and $k$, the exponential regression curve was plotted from Eq. 1 through the $\bar{F}(t)$ data. Graphs, generated by the Apple II Plus computer, were plotted on an Epson MX 80 printer.

## Results

### Incorporation of DTAF-Tubulin into Spindle Fibers

For the experiments reported here pro-metaphase and metaphase cells were microinjected with 5–10% of the cell volume of DTAF-tubulin at a concentration of ~60 μM. After injection, cells were allowed to equilibrate at 32–37°C for 10 min and were then located in the fluorescence microscope. Within this period, steady-state tubulin incorporation into the spindle fibers was nearly complete as determined by the following photometric measurements. At 10 min post-injection, the intensity of fluorescence in the central region of a metaphase half-spindle was measured at 32°C using a laser beam diameter of 2.8 μm. Typically, spindle fluorescence was 6,000 pps compared with 1,500 pps in the adjacent cytoplasm. Next, the cells were cooled to 4°C for 10 min to induce microtubule disassembly. The cells were then rewarmed to 37°C for 10 min to reassemble spindle microtubules from the cytoplasmic pool of unlabeled and DTAF-labeled subunits. The fluorescence in the half-spindle was again measured and compared with the fluorescence intensity measured before cooling and re-warming. The value measured 10 min post-injection was on average 86 +/− 9% ($n$ = 8) of the value obtained after cooling and re-warming. These experiments confirm that incorporation of fluorescent tubulin into spindle fibers is rapid (8, 33, 34) and demonstrate that incorporation throughout the spindle fiber microtubules occurs to near steady-state levels within 10 min.

### Bleached Bar Patterns Do Not Translocate during FRAP

A major prediction of the treadmilling model for mitosis is that microtubules in each half-spindle continually flow or treadmill poleward. This treadmilling action would result from assembly of microtubules at the equatorial region of the spindle and disassembly, at an equal rate, at the spindle poles (19, 20). We have tested this prediction by photobleaching a narrow bar pattern across half-spindles in cells previously injected with fluorescent tubulin. Cells were positioned so that the bleach pattern was perpendicular to the pole-to-pole spindle axis. If a treadmilling mechanism operates during mitosis, then one would expect a translocation of the bleached region poleward, as diagrammed in Fig. 1.

The result of a typical bar pattern bleach experiment is illustrated in Fig. 2. At the start of the experiment, the metaphase BSC 1 spindle (average pole-to-pole length = 22.5 μm) appears uniformly fluorescent (Fig. 2*a*). Immediately after bleaching (Fig. 2*b*), an area of reduced fluorescence is observed across the half-spindle. In most cells, recovery of fluorescence is substantially complete within 2 min (Fig. 2, *c–e*). In addition, because the bar bleach pattern extended completely across the half-spindle, recovery of fluorescence could not occur by lateral displacement of adjacent, unbleached microtubules into the bleached area. Out of a total of 38 experiments with BSC 1 cells, no translocations of the 1.6-μm-wide bar bleach pattern were detected during fluorescence recovery as described in Fig. 1.

In several experiments using BSC 1 cells, a faint image of the bleached region could be seen for ~300 s after bleaching. This observation suggested that FRAP in metaphase spindles was incomplete. This "persistent" bleached fluorescence (on average 25% of the total bleached fluorescence, see below), which we attribute to the differentially stable kinetochore fiber microtubules (3, 25, 30), also appeared stationary during this time.

We also used newt lung epithelial cells in the bar bleach experiment. Because of their large spindle size (average pole-to-pole length = 30 μm), translocations of the bar bleach pattern during FRAP would be easier to detect in these spindles. In addition, the average half-time for fluorescence recovery in these cells is longer than in BSC 1 cells (75 s vs. 37 s) (Wadsworth, P., and E. D. Salmon, unpublished obser-

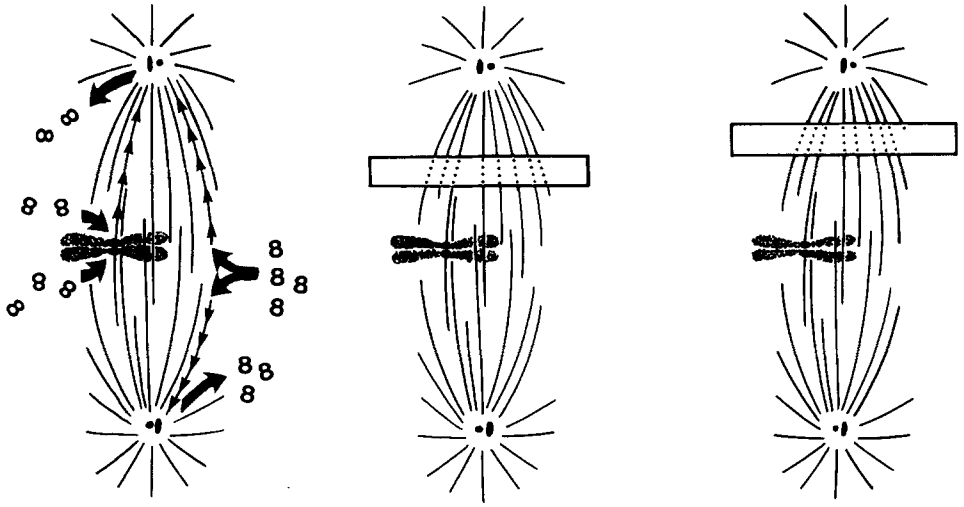

*Figure 1.* Behavior of bar bleach pattern as predicted by the treadmilling model. Arrows mark the sites of tubulin subunit addition to microtubules as proposed in the treadmilling model. The bleached region is represented by the hatched box. With time, the bleached region is translocated poleward by tubulin treadmilling through the microtubules.

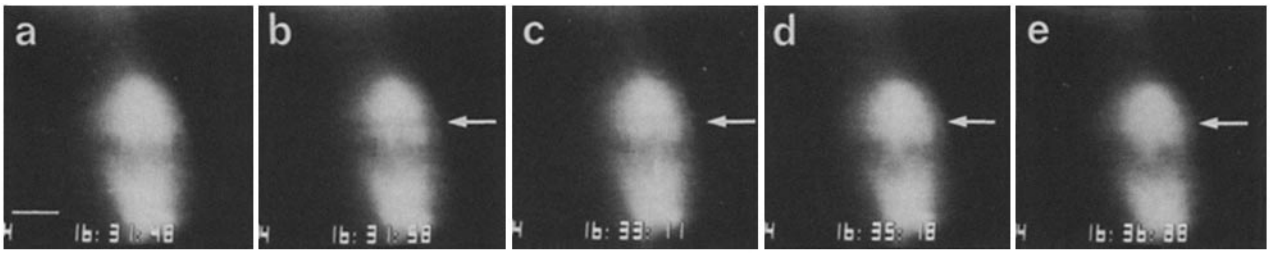


*Figure 2.* Fluorescence recovery after photobleaching of a metaphase BSC 1 cell microinjected with DTAF–tubulin. Spindles were photobleached in a region midway between the chromosomes and the pole for 100 ms using the 488-nm line from an argon ion laser. The bar bleach pattern (1.6-$\mu$m width) was produced by focusing the laser beam at the field diaphragm plane of the epi-illuminator through a cylindrical lens (see Materials and Methods for instrumentation details). Cell before bleaching (*a*), immediately after bleaching (*b*), and after 73 (*c*), 200 (*d*), and 271 (*e*) s of recovery. Arrows mark the position of the bleached region. Bar, 10 $\mu$m.

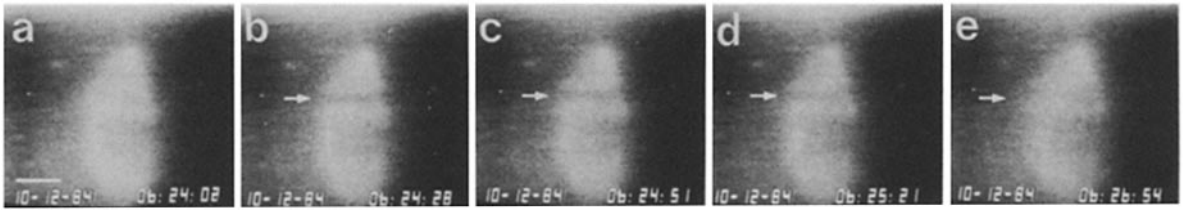


*Figure 3.* Fluorescence recovery after photobleaching of a metaphase newt lung epithelial cell. Experimental details as in Fig. 2. Cell before photobleaching (*a*), immediately after photobleaching (*b*), and after 23 (*c*), 53 (*d*), and 146 (*e*) s of recovery. A faint, stationary line can be seen in all frames, above the bar bleach pattern. This line is due to a defect in the video camera and is not produced by photobleaching. Arrows mark the position of the bleached region. *Bar*, 10 $\mu$m.

vation), increasing the temporal resolution of these experiments. As seen in Fig. 3, however, fluorescence recovery occurs in the bleached region with no detectable translocation of the bar bleached pattern either toward or away from the spindle pole.

How much poleward translation of the bar bleach pattern would be expected if a treadmilling mechanism was responsible for FRAP? If treadmilling were to occur at the rate of anaphase chromosome movement (19, 20) for BSC 1 cells (~1.5 $\mu$m/min at 32°C) or newt lung epithelial cells (~1 $\mu$m/min at 23°C), then the extent of the transloction of the bleached region after photobleaching would be a function of the time after bleaching. For example, at 120 s after bleaching, the interval during which the majority of FRAP occurs, a 2–3-$\mu$m translocation would have occurred (2 min × 1–1.5 $\mu$m/min). This distance is 1.5–2 times the width of our 1.6-$\mu$m bar bleach pattern and would be apparent in our photographs.

### *Rate of FRAP Is Independent of the Size of the Bleached Region*

Photometric measurements of FRAP in circular bleached regions of the half-spindle were next used to determine more accurately the rate and extent of FRAP in BSC 1 cells. In addition, such photometric measurements can be used to determine if flow occurs during recovery by comparing the rate of FRAP in circular bleached regions of two different diameters. If FRAP is produced by a poleward flow of tubulin subunits within half-spindle microtubules, then the recovery curves will display a sigmoid shape as the circular bleached region translates out of the circular measuring beam and the rate of fluorescence recovery will be inversely proportional to the beam diameter (14).

Typical computer records of FRAP obtained by photometric measurements are shown in Fig. 4. The rapid recovery of fluorescence occurred in at least two phases (33). The first phase is due to tubulin diffusion in the cytosol, in the spindle and cytoplasm along the optical path of the laser beam through the cell (29, 32). It is complete within a few seconds after bleaching. This diffusion phase is a minor component of FRAP in these flat cells and is not apparent using the time scale shown in Fig. 4. Similar rates of FRAP due to tubulin diffusion have also been independently measured by bleaching the cytoplasm outside of the microtubule-containing spindle region and measuring FRAP using photometric (data not shown) or video techniques (32).

The major portion of the second phase of fluorescence recovery closely followed an exponential function, and is referred to as the fast incorporation phase of recovery (Fig. 4). In BSC 1 metaphase spindles this fast incorporation phase had a first order rate constant, $k$, of ~0.0195 and a corresponding half-time of fluorescence recovery of ~37 s (Table I). This fast incorporation phase appeared complete by 225 s. Fluorescence recovery of the fast incorporation phase accounted for ~75% of the initial bleached spindle fluorescence. The remaining 25% of the initial bleached fluorescence recovered relatively slowly, if at all, over the time course of these experiments (see Fig. 4). These observations suggest that two different rates of spindle fiber incorporation can occur in these cells, with the faster phase accounting for the majority of the fluorescence recovery (see Fig. 4). A minor portion of the half-spindle microtubules exchange subunits much more slowly than the majority of half-spindle microtubules. The slower incorporation phase has not been included in the rate calculations presented here and has not been analyzed beyond the 385-s sampling period.

A schematic representation of FRAP experiments using two different bleach spot diameters is shown in Fig. 5 and the results of these photometric measurements are presented in Fig. 4 and Table I. For bleach spot diameters of 2.8 and 4.5 $\mu$m, the kinetics of FRAP were identical: (*a*) the fast incor-

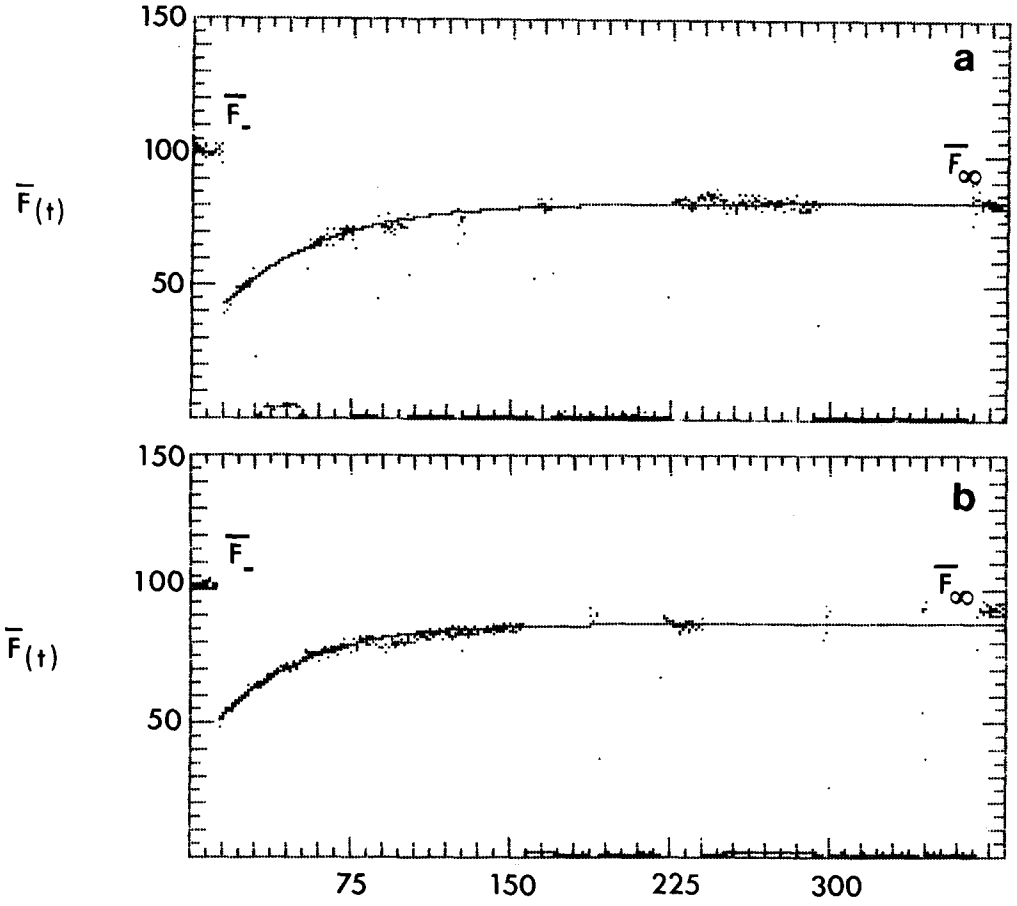


*Figure 4.* Computer records of FRAP for metaphase BSC 1 spindles obtained by photometric measurements. (*a*) Record of FRAP obtained with a bleach spot diameter of 4.5 μm. The half-time for recovery was 33 s and the percentage of bleached fluorescence recovered at 225 s was 68%. (*b*) Record of FRAP obtained with a bleach spot diameter of 2.8 μm. The half-time for recovery was 32 s and the percentage of bleached fluorescence at 225 s was 74%. $\bar{F}_-$ average initial fluorescence; $\bar{F}_\infty$ average fluorescence at 225 s after bleaching. The line through the data points was generated as described in Materials and Methods.

*Table I. FRAP as a Function of Bleach Spot Diameter*

| Spot Diameter | k ($sec^{-1}$)* | $t_{\frac{1}{2}}$* | %R* | *n* |
|---|---|---|---|---|
| 2.8 μm | 0.019 ± .004 | 39 ± 9 | 76 ± 16 | 8 |
| 4.5 μm | 0.020 ± .004 | 36 ± 7 | 75 ± 15 | 9 |

* Determined by exponential regression analysis of recovery curves by plotting ln [$\bar{F}\infty - \bar{F}(t)$] vs. time after photobleaching, as described in Materials and Methods.

poration phase of fluorescence recovery was always exponential, not sigmoidal; (*b*) the half-times of the fast incorporation phase were the same; and (*c*) the percentage of bleached fluorescence recovered was also the same.

## Discussion

The major conclusion of the experiments presented here is that a uniform, poleward flow of tubulin subunits is not the mechanism responsible for fluorescence recovery in the majority of half-spindle microtubules in metaphase BSC 1 and newt lung epithelial cells. Because the treadmilling model predicts that all the microtubules in the half-spindle treadmill poleward (19, 20), our results are inconsistent with such a model. Rather the exponential recovery process observed here

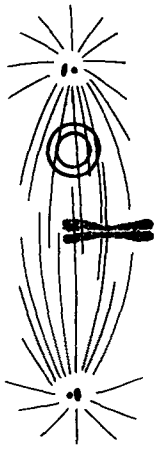

*Figure 5.* Diagram, approximately to scale for an average BSC 1 spindle, of the two spot size experiment. The bleaching beam diameters are 2.8 and 4.5 μm. Bleaches were made in the half-spindle midway between the chromosomes and pole and recovery was measured photometrically.

(Fig. 4), which is independent of bleach spot diameter (Table I), suggests that FRAP occurs by association–diassociation reactions between spindle microtubules and tubulin subunits that occur throughout the spindle at steady-state.

Our conclusions, however, are limited to that fraction of spindle microtubules which recover fluorescence during the time course of our experiments. As seen in Table I, only

~75% of the original fluorescence is recovered in 385 s at 31–33°C. Our interpretation of this incomplete recovery of fluorescence is that a minor fraction of the microtubules in the half-spindle are much more stable than the majority of microtubules. Previous work on a variety of spindle types has shown that kinetochore fiber microtubules are differentially stable to physical and chemical agents that promote microtubule depolymerization (3, 25, 30). The incomplete FRAP observed here, along with the indication of fast and slow rates of fluorescence incorporation during recovery (Fig. 4), suggest that the more stable kinetochore fiber microtubules may recover fluorescence more slowly than the nonkinetochore microtubules. Furthermore, we have been unable to detect any translocation of that fraction of bleached fluorescence which is not recovered during these experiments.

While a continual, uniform flow of subunits toward the spindle pole in the majority of half-spindle microtubules is not supported by the results presented here, several modifications of the treadmilling model can be considered. First, the fraction of differentially stable microtubule polymer may treadmill. Although we have not been able to detect any translocation of the "persistent" bleached fluorescence, this behavior would be difficult to detect against the majority of nontreadmilling polymer in the half-spindle. Secondly, microtubules may treadmill asynchronously, not uniformly. Thirdly, microtubule treadmilling may occur only at certain stages of mitosis, such as during anaphase. At present, we cannot exclude any of these possibilities. Additional experiments, which can resolve the behavior of individual microtubules during all stages of mitosis, are necessary to clarify these issues.

The results of other recent FRAP experiments also support the conclusion that uniform treadmilling of microtubules is not the mechanism responsible for fluorescence recovery. Circular bleach patterns on interphase microtubule arrays, using either DTAF–tubulin or fluorescein-labeled microtubule-associated proteins as the fluorescent probe molecule, recover fluorescence uniformly, without a translocation of the bleached region (34, 35). Video FRAP analysis of circular bleaches in mitotic spindles of sea urchin embryos and $PtK_1$ cells also show a uniform recovery of fluorescence (33, 34).

In the experiments presented here, we have measured tubulin exchange with microtubule polymer at metaphase when the amount of microtubule polymer remains constant. Furthermore, a variety of control experiments demonstrate that the FRAP technique does not destroy microtubule structure (33, 34). This is in contrast to the UV microbeam technique used by Forer (6) to create areas of reduced birefringence (ARBs) on spindle fibers. In Forer's experiments, poleward movements of the ARBs along kinetochore fibers were reported to occur during both metaphase and anaphase in insect spermatocytes. Because a UV microbeam can cause microtubule destruction (15), the UV microbeam experiments are not steady-state measurements of tubulin–microtubule exchange. At present, the molecular mechanism responsible for the apparent poleward movement of ARBs is not known, but the nature of the technique suggests the possibility that repolymerization or repair may be involved.

If FRAP does not occur by synchronous treadmilling, what alternative mechanism might be responsible for the rapid tubulin exchange with the majority of spindle microtubules at steady-state? Simple equilibrium exchange of tubulin subunits at only the ends of steady-state microtubules (24) is not sufficiently rapid to account for the rate of FRAP measured in this and previous studies of mitotic microtubules (33, 34; see also reference 31 for discussion). Alternatively, exchange sites could occur all along the length of half-spindle microtubules, as originally suggested in the Inoué dynamic equilibrium model (10, 11) and more recently from images obtained using cryo-electron microscopy (17). Alternatively, microtubules could be rapidly breaking and reannealing.

Recently, however, Soltys and Borisy (39) have observed that incorporation of fluorescent tubulin into individual cytoplasmic microtubules occurred primarily by growth at the ends of pre-existing microtubules and by the polymerization of new microtubules from the centrosome. Areas of fluorescence were not observed at multiple sites along the length of the microtubules. These observations do not provide direct information on the dynamics of spindle microtubules, but do suggest that the primary sites for tubulin assembly and disassembly are at the ends of microtubules as observed in vitro. One possible means to reconcile the very dynamic behavior of microtubules in living cells with end-dependent growth is that microtubules can rapidly assemble and then disappear in an asynchronous manner. Such a phenomenon, termed "Dynamic Instability," has been described recently by Mitchison and Kirschner for microtubule-associated protein–free microtubules assembled in vitro (22, 23). Rapid asynchronous microtubule elongation and depolymerization, for the majority of half-spindle microtubules, would be in accord with the rapid rate of tubulin turnover measured in spindle fibers of living mitotic cells using FRAP. In addition, a stochastic process would not result in a uniform, directional recovery process, in accord with the results presented here. This model does provide a mechanism whereby end-dependent events are sufficiently rapid to account for in vivo observations providing that the rate of microtubule elongation is sufficiently rapid (29, 31). Recently, we have analyzed the rate and pattern of non–steady-state depolymerization of individual astral microtubules in human monocytes by blocking assembly with nocodazole (4). In these cells, the behavior of each individual microtubule can be quantitated, using immunofluorescence techniques. Our results demonstrate that individual microtubule behavior in living cells can be both rapid and asynchronous as predicted by the Dynamic Instability model.

In conclusion, our experiments demonstrate that the majority of microtubules in a metaphase half-spindle do not synchronously treadmill poleward. Our results are compatible with both the Dynamic Equilibrium model (10, 11), in which the site of assembly is not restricted to the microtubule ends, or the Dynamic Instability model (22, 23), in which assembly of some microtubules and disassembly of others occurs stochastically throughout the microtubule array. Analysis of individual spindle microtubules will be necessary to elucidate the mechanism of microtubule assembly in vivo.

We would like to thank Drs. M. C. Beckerle, K. Jacobson, and T. S. Hays for reading critically this manuscript, and N. Salmon for invaluable editorial assistance. We thank M. Tioran, B. Sims, Drs. Y.-L. Wang and K. Jacobson for technical assistance, and Dr. L. Jamison for assistance with computer programming. Drs. C. Rieder and R. Hard are acknowledged for supplying necessary details concerning primary culture of newt cells. We thank B. Neighbor for BSC 1 cells and our colleagues at the University of North Carolina and Dr. J. R.

McIntosh's laboratory for stimulating discussions. We are particularly indebted to Drs. S. Inoué and G. Ellis for the long-term loan of an inverted, vertical optical bench microscope onto which we constructed our fluorescence photobleaching and recording system, and to Mr. E. Horn for his superb machining of critical components. We appreciate timely equipment loans from Carl Zeiss Co. and Dage Camera.

This work was supported by a National Institute of Health grant (GM24364) to E. D. Salmon and a National Institutes of Health postdoctoral fellowship to P. Wadsworth.

Received for publication 2 July 1985, and in revised form 27 November 1985.

### *References*

1. Axelrod, D., D. E. Koppel, J. Schlesinger, E. Elson, and W. W. Webb. 1976. Mobility measurement by analysis of fluorescence photobleaching recovery kinetics. *Biophys. J.* 16:1055–1069.

2. Bergen, L. G., and G. G. Borisy. 1980. Head-to-tail polymerization of microtubules in vitro. Electron microscope analysis of seeded assembly. *J. Cell Biol.* 84:141–150.

3. Brinkley, B. R., and J. Cartwright. 1971. Ultrastructural analysis of mitotic spindle elongation in mammalian cells in vitro. Direct microtubule counts. *J. Cell Biol.* 50:416–431.

4. Cassimeris, L. U., P. Wadsworth, M. Torian, and E. D. Salmon. 1985. Dynamic instability of cytoplasmic microtubules in vivo. *J. Cell Biol.* 101(5, Pt. 2):24a. (Abstr)

5. Euteneur, U., and J. R. McIntosh. 1981. Structural polarity of kinetochore microtubules in $PtK_1$ Cells. *J. Cell Biol.* 89:338–345.

6. Forer, A. 1965. Local reduction of spindle fiber birefringence in living Nephrotoma sutarales (Loew) spermatocytes induced by ultraviolet microbeam irradiation. *J. Cell Biol.* 25:96–117.

7. Graessmann, A., M. Graessmann, and C. Mueller. 1980. Microinjection of early SV40 DNA fragments and T antigen. *Methods Enzymol.* 65:816–825.

8. Hamaguchi, Y., M. Toriyama, H. Sakai, and Y. Hiramoto. 1985. Distribution of fluorescently labeled tubulin injected into sand dollar eggs from fertilization through cleavage. *J. Cell Biol.* 100:1262–1272.

9. Inoue, S. 1961. Polarizing microscope: design for maximum sensitivity. *In* The Encyclopedia of Microscopy. G. L. Clarke, editor. Reinnold. 480–485.

10. Inoué, S., and H. Sato. 1967. Cell motility by labile association of molecules. *J. Gen. Physiol.* 50:259–292.

11. Inoué, S., and H. Ritter, Jr. 1975. *In* Molecules and Cell Movement. S. Inoué and R. E. Stephens, editors. Raven Press, New York. 3–30.

12. Jacobson, K., Z. Dersko, E.-S. Wu, and G. Poste. 1976. Measurement of the lateral mobility of cell surface components in single, living cells by fluorescence recovery after photobleaching. *J. Supramol. Struct.* 5:565–567.

13. Keith, C. H., J. R. Feramisco, and M. Shelanski. 1981. Direct visualization of fluorescein-labeled microtubules in vitro and in microinjected fibroblasts. *J. Cell. Biol.* 88:234–240.

14. Koppel, D. E., D. Axelrod, J. Schlessinger, E. L. Elson, and W. W. Webb. 1976. Dynamics of fluorescence marker concentration as a probe of mobility. *Biophys. J.* 16:1315–1329.

15. Leslie, R. J., and J. D. Pickett-Heaps. 1984. Spindle microtubule dynamics following ultraviolet microbeam irradiations of mitotic diatoms. *Cell.* 36:717–727.

16. Leslie, R. J., W. M. Saxton, T. J. Mitchison, B. Neighbors, E. D. Salmon, and J. R. McIntosh. 1984. Assembly properties of fluorescein-labeled tubulin in vitro before and after fluorescence bleaching. *J. Cell Biol.* 99:2146–2156.

17. Mandelkow, M.-E., and E. Mandelkow. 1985. Unstained microtubules studied by cryo-electron microscopy. Substructure, supertwist and disassembly. *J. Mol. Biol.* 181:123–135.

18. Margolis, R. L., and L. Wilson. 1978. Opposite end assembly and disassembly of microtubules at steady state *in vitro*. *Cell.* 13:1–8.

19. Margolis, R. L., L. Wilson, and B. I. Kiefer. 1978. Mitotic mechanism based on intrinsic microtubule behavior. *Nature* (*Lond.*) 272:450–452.

20. Margolis, R. L., and L. Wilson. 1981. Microtubule treadmills—possible molecular machinery. *Nature* (*Lond.*) 293:705–711.

21. McIntosh, J. R., W. M. Saxton, D. L. Stemple, R. J. Leslie, and M. J. Welsh. 1985. Dynamics of tubulin and calmodulin in the mammalian mitotic spindle. *Ann. NY Acad. Sci.* In press.

22. Mitchison, T., and M. Kirschner. 1984. Dynamic instability of microtubule growth. *Nature* (*Lond.*) 312:237–242.

23. Mitchison, T., and M. Kirschner. 1984. Microtubule assembly nucleated by isolated centrosomes. *Nature* (*Lond.*) 312:232–237.

24. Purich, D. L., and D. Kristofferson. 1984. Microtubule assembly: a review of progress, principles and perspectives. *Adv. Protein Chem.* 36:133–211.

25. Rieder, C. L. 1981. the structure of the cold-stable kinetochore fiber in metaphase PtK cells. *Chromosoma* (*Berl.*). 84:145–158.

26. Rieder, C. L., and A. S. Bajer. 1977. Effect of elevated temperature on spindle microtubules and chromosome movements in cultured newt lung cells. *Cytobios.* 18:201–234.

27. Rose, G. G., C. M. Pomerat, T. O. Shindler, and J. B. Trunnell. 1958. A cellophane strip technique for culturing tissue in multipurpose culture chambers. *J. Biophys. and Biochem. Cytol.* 4:761–764.

28. Salmon, E. D. 1975. Spindle microtubules: thermodynamics of in vivo assembly and role in chromosome movement. *Ann. NY Acad. Sci.* 253:383–406.

29. Salmon, E. D. 1984. Tubulin dynamics in microtubules of the mitotic spindle. *In* Molecular Biology of the Cytoskeleton. G. G. Borisy, D. W. Cleveland, and D. BV. Morphy, editors. Cold Spring Harbor Laboratory. 99–109.

30. Salmon, E. D., and D. A. Begg. 1980. Cold-stable microtubules in kinetochore fibers of insect spermatocytes during anaphase. *J. Cell Biol.* 85:853–865.

31. Salmon, E. D., M. McKeel, and T. Hays. 1984. Rapid rate of tubulin dissociation from microtubules in the mitotic spindle in vivo measured by blocking polymerization with colchicine. *J. Cell Biol.* 99:1066–1075.

32. Salmon, E. D., W. M. Saxton, R. J. Leslie, M. L. Karow, and J. R. McIntosh. 1984. Diffusion coefficient of fluorescein-labeled tubulin in the cytoplasm of embryonic cells of a sea urchin: video image analysis of fluorescence redistribution after photobleaching. *J. Cell Biol.* 99:2157–2164.

33. Salmon, E. D., R. J. Leslie, W. M. Saxton, M. L. Karow, and J. R. McIntosh. 1984. Spindle microtubule dynamics in sea urchin embryos: analysis using a fluorescein-labeled tubulin and measurements of fluorescence redistribution after laser photobleaching. *J. Cell Biol.* 99:2165–2174.

34. Saxton, W. M., D. L. Stemple, R. J. Leslie, E. D. Salmon, M. Zavortink, and J. R. McIntosh. 1984. Tubulin dynamics in cultured mammalian cells. *J. Cell Biol.* 99:2175–2186.

35. Scherson, T., T. E. Kreis, J. Schlesinger, U. Z. Littauer, G. G. Borisy, and B. Geiger. 1984. Dynamic interactions of fluorescently labeled microtubule-associated proteins in living cells. *J. Cell Biol.* 99:425–434.

36. Shelanski, M. L., F. Gaskin, and C. R. Cantor. 1973. Microtubule assembly in the absence of added nucleotides. *Proc. Natl. Acad. Sci. USA.* 70:765–768.

37. Schneider, M. B., and W. W. Webb. 1981. Measurement of submicron laser beam radii. *Applied Optics.* 20:1382–1388.

38. Sloboda, R. D., W. L. Dentler, and J. L. Rosenbaum. 1976. Microtubule associated proteins and the stimulation of tubulin assembly *in vitro*. *Biochemistry.* 15:4497–4505.

39. Soltys, B., and G. G. Borisy. 1985. Polymerization of tubulin in vivo: direct evidence for assembly onto microtubule ends and from centrosomes. *J. Cell Biol.* 100:1682–1689.

40. Taylor, D. L., P. A. Amato, K. Luby-Phelps, and P. McNeil. 1984. Fluorescent analog cytochemistry. *Trends Biochem. Sci.* 9:88–91.

41. Telzer, B. R., and L. T. Haimo. 1981. Decoration of spindle microtubules with dynein: evidence for uniform polarity. *J. Cell Biol.* 89:373–378.

42. Wadsworth, P., and R. D. Sloboda. 1984. Modification of tubulin with the fluorochrome 5-(4,6-dicheorotriazin-2-YL) amino fluorescein and the interaction of the fluorescent protein with the isolated meiotic apparatus. *Biol. Bull.* 166:357–367.

43. Yguerabide, J., J. A. Schmidt, and E. E. Yguerabide. 1982. Lateral mobility in membranes detected by fluorescence recovery after photobleaching. *Biophys. J.* 39:69–75.